Nuclear Physics **A480** (1988) 175–187
North-Holland, Amsterdam

BETA DECAY RATES OF sd-SHELL NUCLEI IN STELLAR INTERIORS

T. KAJINO[1], E. SHIINO[1] and H. TOKI[1]

National Superconducting Cyclotron Laboratory, Michigan State University, East Lansing, MI 48824-1321, USA

B.A. BROWN

National Superconducting Cyclotron Laboratory and Department of Physics and Astronomy, Michigan State University, East Lansing, MI 48824-1321, USA

B.H. WILDENTHAL

Department of Physics and Astronomy, University of New Mexico, Albuquerque, NM 87131, USA

Received 28 September 1987

Abstract: Gamow–Teller matrix elements of sd-shell nuclei relevant for stellar evolution of massive stars are calculated by using the sd-shell model wave functions of Wildenthal. Emphasis is placed on the calculations of GT transitions between excited states, which are not obtainable by experiment. Our results are compared with the previous work by Fuller *et al.* and are found notably different in many cases. The beta decay rates, as calculated with and without the contributions of excited states, are demonstrated to be quite different under conditions of high density and high temperature.

1. Introduction

One of the most challenging problems in astrophysics is to understand stellar evolution. The evolution of stars with masses $M < 8M_{\odot}$ is believed to stop at a certain stage, such that they become white dwarfs [1]). More massive stars ($M > 8M_{\odot}$) continue their evolution by the burning of heavier elements (oxygen and heavier), a process which eventually leads to a supernova explosion [1]). Heavy elements are believed to be synthesized in the massive stars and are brought into free space by means of the supernova explosions and the stellar wind. Stellar evolutions and heavy-element synthesis are strongly dependent on nuclear reaction rates. In addition to radiative capture of nucleons and alpha particles, weak (beta-decay) processes become important in the oxygen burning stage and later. In these stages, the temperatures and densities become high, the relevant values being $0.1 < T_9 < 5$ and $10^5 \leq \rho/\mu_e \leq 10^9$ [refs. [1,2])]. As the temperature rises, excited nuclear states become populated and beta transitions from excited states contribute to the weak decay rates. As the density rises, electron-capture transitions into additional nuclear excited states become possible. Electron capture changes the electron density and strongly influences the later stages of stellar evolution.

Fuller, Fowler and Newman (FFN) [2]) have made detailed studies of the weak decay rates of sd-shell nuclei which are relevant for stellar evolution. They used the

[1] Present address: Department of Physics, Tokyo Metropolitan University, Setagaya, Tokyo 158, Japan.

0375-9474/88/$03.50

experimental data available at that time together with results obtained from the shell-model wave functions of Chung and Wildenthal [3]) (when these were available) and, as well, on simpler shell-model estimates. Since the FFN work, more experimental data have been accumulated and the shell model of sd-shell nuclei has been developed further by Wildenthal [4]). These new shell-model wave functions have been successfully tested for a wide variety of observables [4-6]). In particular, Brown and Wildenthal [6]) have made a detailed comparison of experimentally observed Gamow-Teller beta decay rates with theory for sd-shell nuclei. With the use of an effective Gamow-Teller operator, the agreement between experiment and theory is impressive. If we compare the experimental data and the shell-model values now available with the FFN values, there are many differences, some as large as one order of magnitude, in the *ft* values. We have therefore decided to calculate Gamow-Teller matrix elements of several nuclei which are relevant for stellar evolution of massive stars [1,2,7]). The beta transitions considered here are $^{26}\mathrm{Al} \rightarrow {}^{26}\mathrm{Mg}$, $^{30}\mathrm{P} \rightarrow {}^{30}\mathrm{Si}$, $^{31}\mathrm{S} \rightarrow {}^{31}\mathrm{P}$, $^{31}\mathrm{P} \rightarrow {}^{31}\mathrm{Si}$, $^{32}\mathrm{S} \rightarrow {}^{32}\mathrm{P}$, $^{33}\mathrm{S} \rightarrow {}^{33}\mathrm{P}$, $^{34}\mathrm{Cl} \rightarrow {}^{34}\mathrm{S}$ and $^{35}\mathrm{Cl} \rightarrow {}^{35}\mathrm{S}$.

This paper is organized as follows. In sect. 2, we summarize the shell-model calculations. In sect. 3 we provide the *ft* values of those nuclei listed above, which include the ones of excited states of parent nuclei up to 1.5 MeV. We then calculate the beta transition rates for a few cases and discuss the role of transitions from excited states of the parent nuclei in sect. 4. A summary of this work is made in sect. 5.

2. Shell model for sd-shell nuclei

We briefly describe here the shell model for sd-shell nuclei and the calculations for the beta-decay *ft* values. The construction of the shell-model wave functions for sd-shell nuclei is described by Wildenthal [4]). In this model, 8 protons and 8 neutrons fill the 0s and 0p orbits completely and the rest are confined to the 1s and 0d orbits. These nucleons occupy all possible sd configurations. The effective model hamiltonian for these calculations was determined empirically. The 63 two-body matrix elements and 3 single-particle energies were assumed as parameters and were fixed by making an iterative least squares fit of shell-model eigenvalues to experimental ground-state binding energies and excitation energies.

The wave functions obtained by diagonalizing this hamiltonian can then be used to calculate various observables [4-6]). Comparisons of such predictions with experiment have confirmed the overall validity of these wave functions and the predictions for other observables can be considered "semi-empirical". The work on Gamow-Teller beta decay is particularly relevant for the present study. All the known beta decay *ft* values have been compared with the shell-model predictions [6]).

The *ft* value is written as

$$ft = 6170/(B(\mathrm{F}) + B(\mathrm{GT}))\,, \tag{1}$$

where $B(\mathrm{F})$ is the reduced transition probability of the Fermi decay and $B(\mathrm{GT})$ is that of the Gamow-Teller decay. They are given by the nuclear matrix elements

$$B(\mathrm{F}) = |\langle f \| \sum_k t_\pm^k \| i \rangle|^2 / (2I_i + 1) , \tag{2}$$

$$B(\mathrm{GT}) = \left(\frac{g_\mathrm{A}}{g_\mathrm{V}}\right)^2 |\langle f \| \sum_k \sigma^k t_\pm^k \| i \rangle|^2 / (2I_i + 1) , \tag{3}$$

with $|g_\mathrm{A}/g_\mathrm{V}| = 1.251$. The Fermi matrix element is expressed simply in terms of the isospin quantum numbers;

$$B(\mathrm{F}) = [T(T+1) - T_{\mathrm{z}i} T_{\mathrm{z}f}] \delta_{\mathrm{if}} , \tag{4}$$

where T is the isospin and $T_{\mathrm{z}i}$ and $T_{\mathrm{z}f}$ are the z-component of the isospin of the initial and the final states, respectively. δ_{if} indicates that the transitions are allowed only between nuclear analog states.

The Gamow-Teller matrix elements require detailed initial and final wave functions. They are provided by the sd-shell model calculation previously described [4]). It is well known that the shell-model $B(\mathrm{GT})$ values exceed the experimental values on the average. The source of the quenching has been investigated [8,9]) and is due to nuclear core polarization and delta isobar excitations. Brown and Wildenthal take into account this effect by modifying the Gamow-Teller matrix elements (4 parameters) so as to fit the experimental $B(\mathrm{GT})$ values. To a good approximation the effect operator amounts to introducing an overall quenching factor γ defined by

$$B(\mathrm{GT})_{\mathrm{eff}} = \gamma^2 B(\mathrm{GT})_{\mathrm{shell\ model}} . \tag{5}$$

$\gamma = 0.77$ provides good overall agreement with experiments [6,7]). We use this overall quenching factor for our comparisons.

3. Beta decay *ft* values

In table 1 we list the beta-decay *ft* values calculated by the shell model for the eight parent-daughter pairs. Since we are interested in the temperature $T_9 \leqslant 5$, we consider excited states of the parent nuclei up to $E_\mathrm{x} = 1.5$ MeV. The excited states above this energy are populated less than 3% at $T_9 = 5$ and can be neglected for the calculation of the transition rates. As for the daughter nuclei, we take excited states up to $E_\mathrm{x} \sim 5$ MeV as far as the spin and parity are known experimentally. Some states, whose spins are not assigned experimentally, are nicely described by the shell model. We include such states in our tabulation, with experimental excitation energies.

When experimental *ft* values are available, they are shown in table 1 in brackets under the theoretical values. When both Fermi and Gamow-Teller transitions are allowed, the combined *ft* values are provided in the table. The comparison of theory with experiment shows very good agreement. The small difference indicates the

TABLE 1

Log ft values for Fermi and Gamow-Teller transitions from initial states (row) to final states (column)

(a) $^{26}_{13}Al \rightarrow ^{26}_{12}Mg$ $q_n = 3.4939$ MeV $T_{1/2} = 7.2 \times 10^5$ year

	f	1	2	3	4	5	6	7	8	9	10	11	12	13	14	15	16	17
	Energy	0	1.8087	2.9384	3.588	3.9409	4.320	4.3323	4.3501	4.835	4.901	4.972	5.2908	5.474	5.690	5.715	6.127 [a])	6.257
i	J^π, T	$0^+, 1$	$2^+, 1$	$2^+, 1$	$0^+, 1$	$3^+, 1$	$4^+, 1$	$2^+, 1$	$3^+, 1$	$2^+, 1$	$4^+, 1$	$0^+, 1$	$2^+, 1$	$4^+, 1$	$1^+, 1$	$4^+, 1$	$3^+, 1$	$0^+, 1$
1	0						5.94				5.62			5.60		8.83		
	$5^+, 0$						[4.10]				[4.10]							
2	0.2282	3.49													6.91			
	$0^+, 1$	(3.489)													[4.19]			
3	0.4169		5.08	4.21		6.17	5.98	5.42	4.87	4.59	9.31		6.06	5.87		6.06		
	$3^+, 0$		[5.17]^{CW}	[4.07]^{CW}		[4.98]	[4.34]	[4.97]^{CW}	[4.98]	[4.78]^{CW}	[4.34]		[4.94]^{CW}					
4	1.0578	4.02	3.85	5.31	5.50			5.07		5.47		6.42	7.41		6.56			5.05
	$1^+, 0$	[3.85]^{CW}	[3.63]^{CW}	[5.49]^{CW}	[5.72]^{CW}			[5.22]^{CW}		[4.87]^{CW}		[7.50]^{CW}	[6.34]^{CW}				[4.83]	

[a] This state is identified $(1^+, 1)$ in FFN. The full sd-shell model predicts $(3^+, 1)$.

(b) $^{30}_{15}P \rightarrow ^{30}_{14}Si$ $q_n = 3.7162$ MeV $T_{1/2} = 2.5$ min

	f	1	2	3	4	5	6	7	8	10	12	15	17	19	20	23	25
	Energy	0	2.2355	3.4982	3.7696	3.7877	4.809	4.8305	5.230	5.372	5.613	6.537	6.640	6.865	6.914	7.079	7.256
i	J^π, T	$0^+, 1$	$2^+, 1$	$2^+, 1$	$1^+, 1$	$0^+, 1$	$2^+, 1$	$3^+, 1$	$3^+, 1$	$0^+, 1$	$2^+, 1$	$2^+, 1$	$0^+, 1$	$3^+, 1$	$2^+, 1$	$3^+, 1$	$2^+, 1$
1	0	4.85	5.79	5.05	6.17	4.463	5.43			5.05	6.54	4.94	5.19		5.84		4.88
	$1^+, 0$	(4.843)	(5.882)	(5.225)	(5.780)	(4.477)											
		[4.83]^{E}	[5.80]^{E}	[4.17]^{CW}	[4.83]	[5.01]^{CW}	[5.33]^{CW}			[4.43]^{CW}							
2	0.6772																
	$0^+, 1$	3.49			5.49												
3	0.7090																
		5.813	5.50	4.37	5.53	7.98	4.93			5.81	5.18	6.12	6.06		4.96		4.94
	$1^+, 0$	(6.18)															
		[6.18]^{E}	[4.58]^{CW}	[5.98]^{CW}	[4.83]	[4.58]^{CW}	[4.43]^{CW}			[4.83]^{CW}							
4	1.454																
	$2^+, 0$		4.61	6.93	4.79		5.01	5.03	4.69		6.81	5.84		4.48	5.38	5.53	6.35
			[4.46]	[4.46]	[4.80]		[4.46]	[4.43]	[4.43]								

(c) $^{31}_{15}P \rightarrow ^{31}_{14}Si$ $q_n = -2.0018$ MeV $T_{1/2} = \infty$

i	f	1	2	3	4	5	9	12	15
	Energy	0	0.7525	1.6951	2.317	2.790	4.259	4.720	5.282
	J^π, T	$\frac{3}{2}^+, \frac{3}{2}$	$\frac{1}{2}^+, \frac{3}{2}$	$\frac{5}{2}^+, \frac{3}{2}$	$\frac{3}{2}^+, \frac{3}{2}$	$\frac{5}{2}^+, \frac{3}{2}$	$\frac{3}{2}^+, \frac{3}{2}$	$\frac{1}{2}^+, \frac{3}{2}$	$\frac{1}{2}^+, \frac{3}{2}$
1	0	5.11	4.59		4.84		4.86	4.07	6.32
	$\frac{1}{2}^+, \frac{1}{2}$	(5.231)							
2	1.2661	5.61	5.61	5.44	5.64	6.06	5.98	6.54	5.35
	$\frac{3}{2}^+, \frac{1}{2}$								

(d) $^{31}_{16}S \rightarrow ^{31}_{15}P$ $q_n = 4.8843$ MeV $T_{1/2} = 2.6$ sec

i	f	1	2	3	4	5	7	8	9	11	13	14	15	16	20	29
	Energy	0	1.2661	2.2338	3.1343	3.2950	3.506	4.191	4.260	4.592	4.783	5.02	5.116	5.257	5.557	6.337
	J^π, T	$\frac{1}{2}^+, \frac{1}{2}$	$\frac{3}{2}^+, \frac{1}{2}$	$\frac{5}{2}^+, \frac{1}{2}$	$\frac{1}{2}^+, \frac{1}{2}$	$\frac{5}{2}^+, \frac{1}{2}$	$\frac{3}{2}^+, \frac{1}{2}$	$\frac{5}{2}^+, \frac{1}{2}$	$\frac{3}{2}^+, \frac{1}{2}$	$\frac{3}{2}^+, \frac{1}{2}$	$\frac{5}{2}^-, \frac{1}{2}$	$\frac{1}{2}^+, \frac{1}{2}$	$\frac{5}{2}^+, \frac{1}{2}$	$\frac{1}{2}^+, \frac{1}{2}$	$\frac{3}{2}^+, \frac{1}{2}$	$\frac{1}{2}^+, \frac{1}{2}$
1	0	3.67 [a]	5.14		4.78		4.39		5.70	5.33		5.15		4.73	5.02	4.59
	$\frac{1}{2}^+, \frac{1}{2}$	(3.685)	(4.966)		(4.768)		(4.579)									
2	1.2489	5.45	3.73 [b]	6.12	6.72	5.17	4.84	4.28	6.04	6.61	8.39	4.68	7.09	5.37	6.00	5.60
	$\frac{3}{2}^+, \frac{1}{2}$															

[a]) Fermi and Gamow-Teller transitions are mixed. GT only provides $\ln ft = 4.44$.
[b]) Fermi and Gamow-Teller transitions are mixed. GT only provides $\ln ft = 4.62$.

(e) $^{32}_{16}S \rightarrow ^{32}_{15}P$ $q_n = -2.2214$ MeV $T_{1/2} = \infty$

i	f	1	2	3	4	9	11	17	25
		0	0.0781	0.5131	1.1498	2.2298	2.741	3.697 [a]	4.203
	J^π, T	$1^+, 1$	$2^+, 1$	$0^+, 1$	$1^+, 1$	$1^+, 1$	$1^+, 1$	$1^+, 1$	$1^+, 1$
1	0	8.11			4.18	5.43	4.85	5.29	3.94
	$0^+, 0$	(7.430)							

[a]) Theory predicts the fifth $(1^+, 1)$ state at $E_x = 3.697$ MeV.

TABLE 1—continued

(f) $^{33}_{16}S \rightarrow {}^{33}_{15}P$ $q_n = -0.760$ MeV $T_{1/2} = \infty$

i	f	1	2	3	4	5	6	8	9
	Energy	0	1.4314	1.8476	2.5376	3.276	3.490	4.048	4.194
	J^π, T	$\frac{1}{2}^+, \frac{3}{2}$	$\frac{3}{2}^+, \frac{3}{2}$	$\frac{5}{2}^+, \frac{3}{2}$	$\frac{3}{2}^+, \frac{3}{2}$	$\frac{3}{2}^+, \frac{3}{2}$	$\frac{5}{2}^+, \frac{3}{2}$	$\frac{5}{2}^+, \frac{3}{2}$	$\frac{5}{2}^+, \frac{3}{2}$
1	0								
	$\frac{3}{2}^+, \frac{1}{2}$	5.46 (5.335)	5.41	5.41	6.24	4.81	5.84	5.64	4.35
2	0.8404								
	$\frac{1}{2}^+, \frac{1}{2}$	4.45	5.33		5.60	5.94			

(g) $^{34}_{17}Cl \rightarrow {}^{34}_{16}S$ $q_n = 4.982$ MeV $T_{1/2} = 1.526$ sec

i	f	1	2	3	4	5	6	8	9	10	11	13	18
	Energy	0	2.127	3.304	3.914	4.072	4.115	4.688	4.875	4.891	5.23	5.39	5.993
	J^π, T	$0^+, 1$	$2^+, 1$	$2^+, 1$	$0^+, 1$	$1^+, 1$	$2^+, 1$	$4^+, 1$	$3^+, 1$	$2^+, 1$	$0^+, 1$	$1^+, 1$	$2^+, 1$
1	0												
	$0^+, 1$	3.49 (3.491)				5.18						5.31	
2	0.146												
	$3^+, 0$		6.56 (5.990)	4.86 (4.832)			5.15 (5.089)	5.59 (5.437)	5.25 (5.190)	5.98			5.90
3	0.461												
	$1^+, 0$	6.34	5.65	4.69	5.52	5.93	8.14			4.99	5.03	6.22	5.54
4	0.666												
	$1^+, 0$	5.35	4.79	5.40	6.47	5.29	5.07			4.94	5.09	6.15	5.32
5	1.230												
	$2^+, 0$		5.40	4.57		4.85	4.61		5.61	5.26		5.12	4.79

(h) $^{35}_{17}\mathrm{Cl} \rightarrow {}^{35}_{16}\mathrm{S}$ $\quad q_n = -0.67848$ MeV $\quad T_{1/2} = \infty$

	f	1	2	5	6	7
		0	1.5722	2.718	2.939	3.421
i	J^π, T	$\frac{3}{2}^+, \frac{3}{2}$	$\frac{1}{2}^+, \frac{3}{2}$	$\frac{5}{2}^+, \frac{3}{2}$	$\frac{3}{2}^+, \frac{3}{2}$	$\frac{5}{2}^+, \frac{3}{2}$
1	0	5.08	5.54	5.42	4.92	4.55
	$\frac{3}{2}^+, \frac{1}{2}$	(5.021)				
2	1.2194	7.76	4.75		5.47	
	$\frac{1}{2}^+, \frac{1}{2}$					

Experimental energies are used for excitation energies. Calculated log ft values are depicted without brackets, while experimental values are given within curly brackets. The numbers in square brackets are those listed in FFN; superscript E denotes experiment, CW the Chung-Wildenthal value, no superscript indicates the simpler shell model estimate.

quality of the shell-model predictions. For two cases, $^{26}\mathrm{Al} \rightarrow {}^{26}\mathrm{Mg}$ and $^{30}\mathrm{P} \rightarrow {}^{30}\mathrm{Si}$, we can compare our *ft* values with those used by FFN. There are many cases, where the *ft* values differ by one order of magnitude. Particularly noteworthy is the transition from the ground state of ^{30}P to the 2_2^+ state at $E_x = 3.50$ MeV of ^{30}Si. The FFN value adopted for the transition rate calculation is $\log ft = 4.17$, while our value is $\log ft = 5.05$. This difference will be important in the transition rates as will be discussed later. As for the case of $^{26}\mathrm{Al} \rightarrow {}^{26}\mathrm{Mg}$, the transitions from the ground state ($I^\pi = 5^+$) to the first and second 4^+ states were estimated by FFN to have $\log ft = 4.10$. On the other hand, our values obtained by the full sd-shell-model calculations are 5.94 and 5.62, respectively. The Gamow-Teller strengths between excited states are not obtained experimentally and we must rely entirely on the shell-model calculation. The detailed comparison of the shell-model predictions with various experimental data provides some confidence in those values given only by the shell model.

4. Transition rates

The transition rate from the *i*th state of the parent to the *j*th state of the daughter nucleus is given by

$$\lambda_{ij} = \ln 2 \frac{f_{ij}(T, \rho, U_F)}{(ft)_{ij}}. \tag{6}$$

$(ft)_{ij}$ is the *ft* value listed in table 1. The experimental *ft* values are used when available, otherwise the new calculated values are used. The expressions for the phase space integral $f_{ij}(T, \rho, U_f)$ with T, ρ and U_F being the temperature, density and the electron chemical potential are provided in FFN [2]). The transition rates from the parent to the daughter nucleus are then calculated by summing over the initial and final states with the population probabilities;

$$\lambda = \sum_{ij} P_i \lambda_{ij}, \tag{7}$$

$$P_i = (2I_i + 1)\, \mathrm{e}^{-E_i/kT} \Big/ \sum_i (2I_i + 1)\, \mathrm{e}^{-E_i/kT}. \tag{8}$$

Here, I_i is the spin of the initial state and E_i the corresponding excitation energy.

We present here some examples of these calculations which illustrate the role of the excited states. Arnett and Thielemann have used the FFN transition rates for the stellar evolution calculations of massive stars [10]). They demonstrate the importance of the weak beta process in the oxygen and silicon burning stages for energy release and neutronization, a small change of which has important effects on both nucleosynthesis and on the dynamic behavior of the final core collapse. Hence, we shall make comparison of our results with those of FFN. Chosen first is the case $^{33}\mathrm{S} \rightarrow {}^{33}\mathrm{P}$ where there is no Fermi transition. The transition rates due to electron capture are shown in fig. 1a as a function of temperature at density $\rho/\mu_e = 10^9$ and

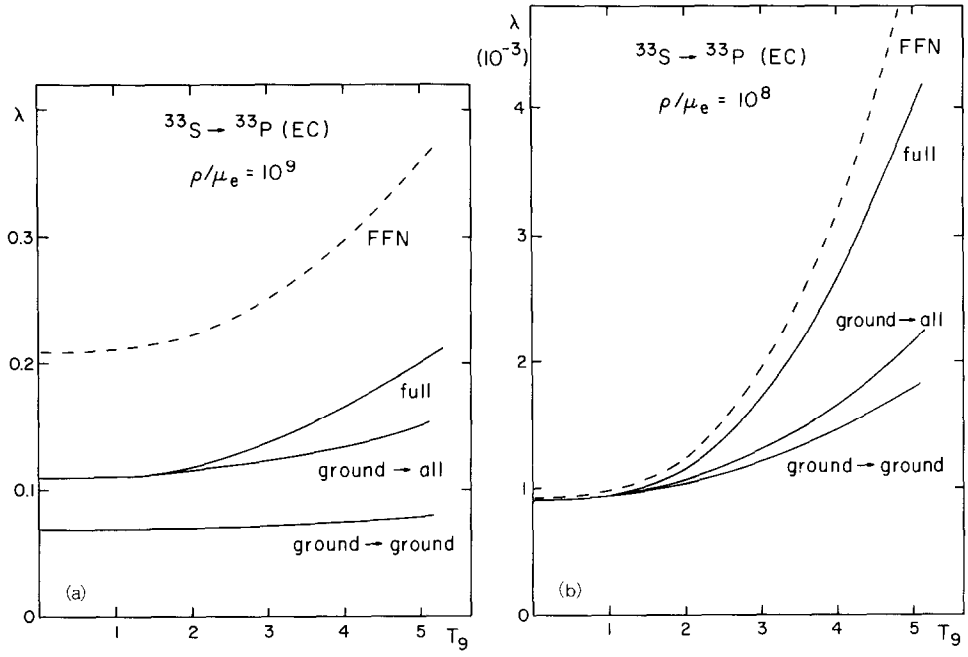

Fig. 1. (a) Transition rates λ due to electron capture for $^{33}S \rightarrow {}^{33}P$ as a function of temperature T_9 at the density 10^9. Limited cases of the ground state to ground state transition and the ground state to all final excited state transitions are those denoted by "ground → ground" and "ground → all" beside the solid lines, respectively. The case with all initial and final state transitions included is denoted by "full". The "full" results of FFN are shown by a dashed line. (b) Transition rates λ due to electron capture for $^{33}S \rightarrow {}^{33}P$ as a function of temperature T_9 at the density 10^8.

10^8. When the transition is limited to the ground-to-ground transition, the rate is almost constant as a function of the temperature. Since the electron Fermi energy, U_F, is high ($U_F \sim 5$ MeV) at these high densities, the excited states of the daughter nucleus become quite important. Inclusion of the excited states of the daughter nucleus, increase the transition rates by 50–100%. The influence of the excited states of the parent nucleus becomes evident as the temperature becomes high ($T_9 \geq 2$). As a comparison, the transition rates, calculated by FFN, are plotted in fig. 1a. The two sets of results are about a factor two different. Since the ground to ground transition is known experimentally, this difference is due to the use of different *ft* values for transitions from the ground state to excited states in the daughter nucleus. A reduction of the density reduces the importance of excited daughter states and reduces the discrepancy. This can be seen in fig. 1b where $\rho/\mu_e = 10^8$ has been used. At this lower density, the role of the excited states of the parent nucleus becomes relatively important as the temperature increases. The full results are now similar to those of FFN.

The next example, shown in fig. 2a, is the case of $^{30}P \rightarrow {}^{30}Si$. At the high density $\rho/\mu_e = 10^9$, the inclusion of the excited states of the daughter nucleus increases the

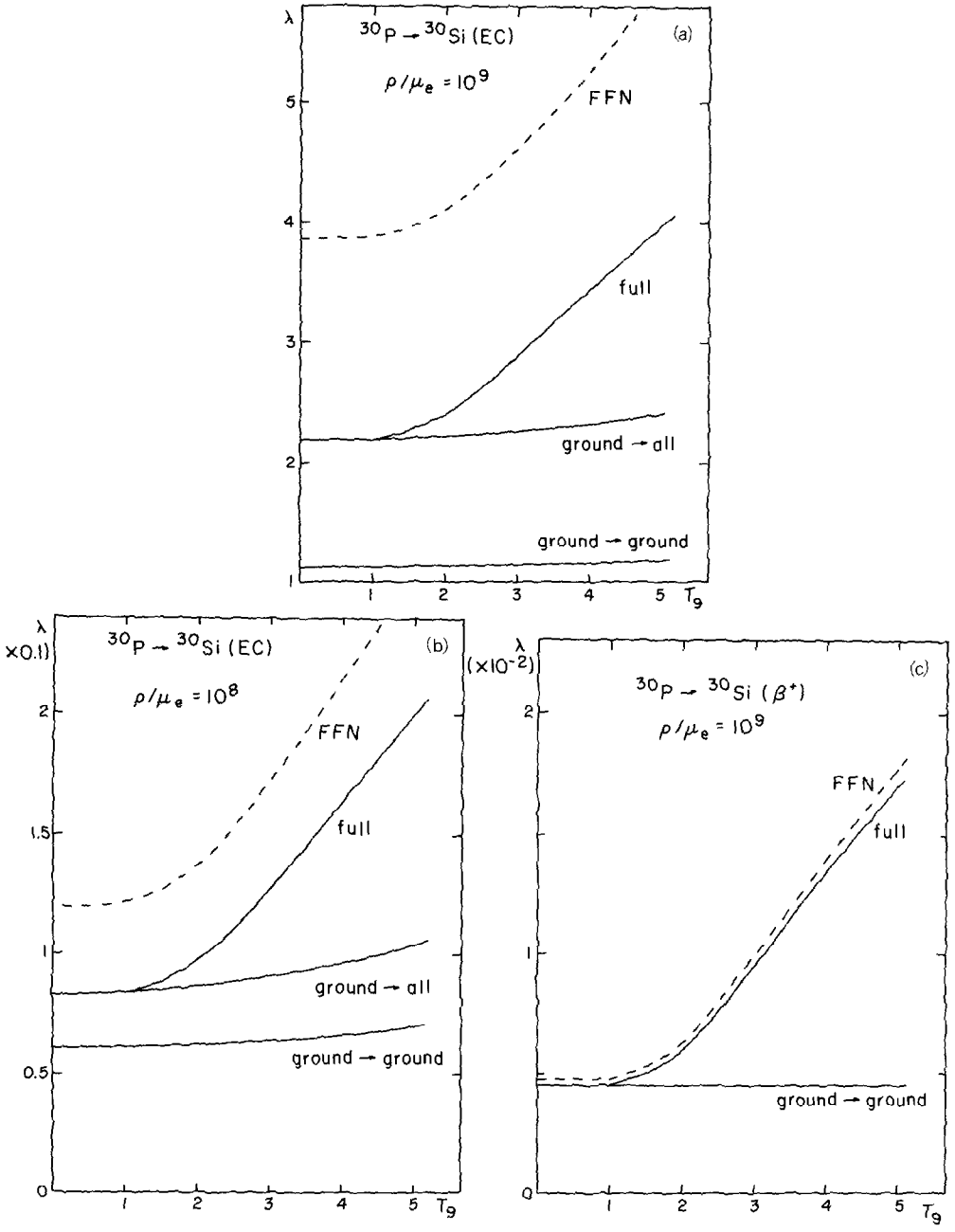

Fig. 2. (a) Transition rates λ due to electron capture for $^{30}P \rightarrow {}^{30}Si$ as a function of temperature T_9 at the density 10^9. The notation is explained in the figure caption for fig. 1a. (b) Transition rates λ at the density 10^8. (c) Transition rates λ due to β^+ decay for $^{30}P \rightarrow {}^{30}Si$ as a function of temperature T_9 at the density 10^9.

transition rate by a factor of two. The inclusion of the excited states in the parent nucleus, in particular the first excited state ($I^{\pi}=0^{+}$, $T=1$), which Fermi decays into the ground state, increases the transition rate as the temperature increases. The transition rates of FFN are much larger than ours. The difference originates from the use of different *ft* values for the transition from the ground state to the second and the third excited states. In fig. 2b, we show the case of lower density $\rho/\mu_e = 10^8$. The qualitative feature remains the same as the high density case. This is because the q_n value ($q_n = M_i - M_f$) is positive for this case and the excited states of the daughter nucleus are populated by beta-decay even at lower density.

We show in fig. 2c the case of β^+ decay for $^{30}P \rightarrow {}^{30}Si$. Our results essentially agree with those of FFN. The sudden increase of the transition rates with temperature is caused by the Fermi transition from the first excited state.

The results on the electron capture for $^{26}Al \rightarrow {}^{26}Mg$ are shown in fig. 3 at $\rho/\mu_e = 10^9$. Our results differ significantly from those of FFN. The difference arises by the use of largely different *ft* values for the Gamow-Teller transitions from the 5^+ ground state to the excited 4^+ states. The sudden increase of the transition rates is again due to the Fermi transition from the first excited state to the ground state.

We have made similar comparison for other cases. Our results and those of FFN differ by similar amounts as the cases discussed here.

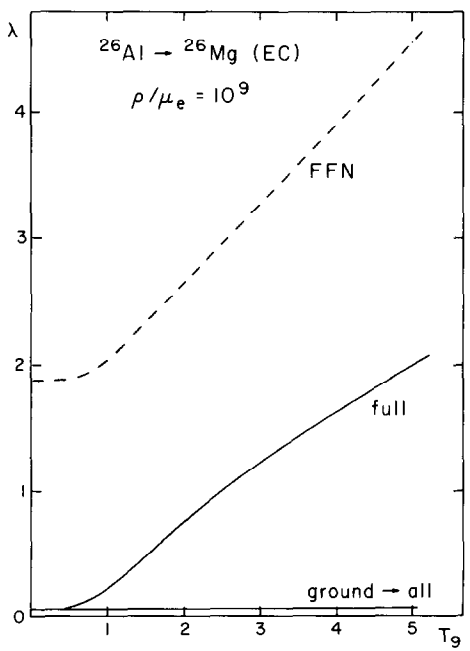

Fig. 3. Transition rates λ due to electron capture for $^{26}Al \rightarrow {}^{26}Mg$ as a function of temperature T_9 at the density 10^9. The notation is explained in the figure caption for fig. 1a.

5. Conclusion

We have calculated weak beta transition *ft* values of sd-shell nuclei relevant for stellar evolution of heavy stars. Our emphasis was placed on the calculation of transitions between excited states of parent and daughter nuclei, which cannot be obtainable from experiment. We have compared the *ft* values with those of FFN. We find that in many cases the *ft* values differ by an order of magnitude. The origins of these differences is the improvement of the shell-model wave functions used to calculate the GT matrix elements.

With the use of the *ft* values, we have calculated the transition rates as functions of temperature and density. The transition rates due to electron capture increase rapidly as the density increases due to electron degeneracy. The role of the beta transitions from the ground state to the excited states is significant in this case. On the other hand, as the temperature becomes high, the excited states of the parent nucleus become populated by the thermal equilibrium process and the beta transitions from the excited states to states in the daughter nucleus become progressively more important.

As far as the comparison with the FFN results go, we find in several cases differences by about a factor two at high temperature and high density. We believe that the predicted *ft* values of the present sd-shell model are more reliable than those estimated by FFN. In order to increase our confidence, however, it would be desirable to perform (n, p) reactions from the stable nuclei (^{31}P, ^{32}S, ^{33}S, ^{35}Cl), the technique for which has now become available. Predicted Gamow-Teller strengths are provided in table 1.

Our studies on the Gamow-Teller transitions are importnat for understanding the stellar evolution at the later stage of heavy stars, in particular heavy nuclear synthesis and the supernova explosions. In addition, β^+ decays in sd-shell nuclei form the main path of the rapid-proton (rp) process in various sites of stellar objects [11]. The present theoretical calculations should be incorporated into detailed studies of the nucleosynthesis calculations. Such calculations are possible by the Santa Cruz group [12], the Livermore group [13] and the Tokyo group [1].

We acknowledge fruitful discussions with Prof. K. Nomoto and Dr. M. Hashimoto at the early stage of this work. We are grateful to Dr. M. Hashimoto for sending us the computer code to calculate the decay rates. We acknowledge the financial support by MSU Cyclotron Laboratory, which made the present study possible.

This research was supported in part by the US National Science Foundation under grant nos. PHY83-12245 and PHY87-18772.

References

1) K. Nomoto and M. Hashimoto, Part. Nucl. Physics, **18** (1986)
2) G.M. Fuller, W.A. Fowler and M.J. Newman, Ap. J. Suppl. **42** (1980) 447; Ap. J. **252** (1982) 715

3) W. Chung, Ph.D. thesis, Michigan State University (1976);
B.H. Wildenthal, Elementary modes of excitation in nuclei, LXIX, Corso, Soc. Italiana di Fisica, Bologna, Italy (1977)
4) B.H. Wildenthal, Progr. Part. Nucl. Phys., vol. 11, ed. D.H. Wilkinson (Pergamon, Oxford, 1984) 5
5) B.A. Brown, Proc. at the Int. Nuclear Physics Conf., Harrogate UK, 25-30 Aug. 1986 (Inst. of Phys. Conf. Series Number 86, Institute of Physics, Bristol) p. 119;
M. Carchidi, B.H. Wildenthal and B.A. Brown, Phys. Rev. **C34** (1986) 2280;
B.H. Wildenthal, B.A. Brown and I. Sick, Phys. Rev. **C33** (1985) 2185
6) B.A. Brown and B.H. Wildenthal, At. Data Nucl. Data Tables, **33** (1985) 347
7) K. Nomoto and M. Hashimoto, private communication
8) B.A. Brown and B.H. Wildenthal, Phys. Rev. **C28** (1983) 2397; Nucl. Phys. **A474** (1987) 290
9) I.S. Towner and F.C. Khanna, Nucl. Phys. **A399** (1983) 334;
E. Oset, H. Toki and W. Weise, Phys. Reports 83 (1982) 281;
A. Arima, K. Shimizu, W. Bentz and H. Hyuga, to be published
10) W.D. Arnett and F.-K. Thielemann, Ap. J. **295** (1985) 589 and 604
11) R.K. Wallace and S.E. Woosley, Ap. J. Supp. **45** (1981) 389
12) S.E. Woosley, W.D. Arnett and D.D. Clayton, Ap. J. **175** (1972) 731;
S.E. Woosley and T.A. Weaver, Essays in nuclear astrophysics, ed. C.A. Barnes, D.D. Clayton and D.N. Schramm, (Cambridge Univ. Press, 1982) p. 377
13) J.R. Wilson, *in* Numerical astrophysics, ed. J. Centrella, J. LeBlanc and R. Bowers (Jones and Bartlett, Boston, 1985) p. 422